Magnetic penetration depth and condensate density of cuprate high-T_c superconductors determined by muon-spin-rotation experiments

C. Bernhard, Ch. Niedermayer, U. Binninger, A. Hofer, and Ch. Wenger
Universität Konstanz, Fakultät für Physik, D-78434 Konstanz, Germany

J. L. Tallon and G. V. M. Williams
Institute for Industrial Research and Development, Box 31310, Lower Hutt, New Zealand

E. J. Ansaldo
TRIUMF, University of British Columbia, Vancouver, British Columbia, Canada V6T 2A3
and University of Saskatchewan, Saskatoon, Canada S7N 0W0

J. I. Budnick
Department of Physics, University of Connecticut, Storrs, Connecticut 06268

C. E. Stronach, D. R. Noakes, and M. A. Blankson-Mills
Department of Physics, Virginia State University, Petersburg, Virginia 23806
(Received 6 February 1995; revised manuscript received 7 June 1995)

We summarize our results of transverse-field muon-spin-relaxation (TF-μSR) experiments on a variety of polycrystalline cuprate high-T_c superconducting systems. In this paper we present the conditions under which the μSR depolarization rate at low temperatures $\sigma_0 \propto \lambda_{ab}^{-2}(0) \propto n_s(0)/m_{ab}^*$ is determined in a unique way by the doping state of CuO_2 planes and the consequent critical temperature T_c. Disorder and pinning effects due to various sorts and amounts of dopant atoms do not affect σ_0. From our results on $YBa_2Cu_3O_{7-\delta}$, $YBa_2Cu_4O_8$, and $Y_2Ba_4Cu_7O_{15-\delta}$ (systems having both planes and chains) we conclude that a superconducting condensate is not only formed in the CuO_2 planes but is induced additionally in the CuO chains. This chain condensate is rapidly suppressed by any disorder in the chains and depends strongly on the oxygen ordering.

I. INTRODUCTION

It is widely accepted that the CuO_2 planes are the essential structural element for superconductivity in the high-T_c cuprates. The critical temperature T_c (Ref. 1) and many of the highly unconventional normal-state electronic properties such as resistivity,[2] thermoelectric power (TEP),[3] Hall effect,[4] and spin susceptibility[5] exhibit a systematic variation with the concentration of charge carriers p_{sh} within the CuO_2 sheets. With increasing p_{sh} the critical temperature T_c first rises in the so-called underdoped regime, then saturates towards the system-dependent maximum ($T_{c,\max}$) at optimum doping before it decreases again on the overdoped side.[1] Even though the normal-state electronic properties are unusual and not yet fully understood, there is growing evidence that they vary systematically with p_{sh}, independent of the different insulating spacer layers. Therefore, these normal-state properties provide a means to determine the doping state p_{sh} of a sample, for example, by TEP measurements.[3]

Transverse-field muon-spin-relaxation (TF-μSR) experiments revealed a remarkable correlation between T_c (and thus p_{sh}) and the "in-plane" magnetic penetration depth λ_{ab}.[6-10] The distribution of the precession frequencies and the resulting depolarization rate σ of the initially polarized muon spins are a very sensitive, local probe for the field profile in the flux-line lattice (FLL) state of type II superconductors which is determined by the magnetic penetration depth λ. The cuprate superconductors are highly anisotropic with $\lambda_c \gg \lambda_{ab}$ and of extreme type II with $\lambda_{a,b,c} \gg \xi_{a,b,c}$. The in-plane penetration depth λ_{ab} is generally assumed to be determined by the density of the superconducting condensate n_s and the effective mass m_{ab}^* of the carriers ($\lambda_{ab}^{-2} \propto n_s/m_{ab}^*$).[6-11] The superfluid response across the insulating spacer layers is very weak and for the strongly anisotropic systems it is probably based mainly on Josephson effects and, therefore, is related to the normal state resistivity for currents across the CuO_2 planes ($\lambda_c^2 \propto \rho_c$).[12-15]

The earliest TF-μSR experiments indicated a unique linear relationship between the depolarization rate at low temperatures σ_0, and T_c in the underdoped regime of the systems $YBa_2Cu_3O_{7-\delta}$ and $La_{2-x}Sr_xCuO_4$:[6]

$$\sigma_0 \propto \lambda(0)_{ab}^{-2} \propto \frac{n(0)_s}{m_{ab}^*} \propto T_c. \tag{1}$$

Around optimum doping where T_c saturates, one finds that $\sigma_0(p_{sh})$ continues to increase with slight overdoping. In the regime of strong overdoping, however, recent μSR experiments on the systems $Tl_2Ba_2CuO_{6+\delta}$ (Refs. 7 and

0163-1829/95/52(14)/10488(11)/$06.00

10) and $(Y,Yb)_{1-x}Ca_x$ $Ba_xCu_3O_{7-\delta}$ (Refs. 8, 9, and 16) show that σ_0 is strongly depressed with further increasing p_{sh} falling more or less linearly with T_c. The existing data imply a generic phase diagram, where T_c versus $n_s(0)/m^*_{ab}$ describes a "boomerang" shaped path with increasing p_{sh} from the underdoped to the heavily overdoped regime. While the reduction of n_s and T_c on the underdoped side can be understood in terms of a decrease of p_{sh}, some other mechanism has to account for the reduction of T_c and n_s in the overdoped regime. An unambiguous identification of the microscopic mechanism(s) behind this phase diagram is still lacking and requires further experimental and theoretical work. At present, however, it may be even more important to point out that this unique behavior is not merely an artifact of an incorrect interpretation of the μSR-data but reflects intrinsic properties of the superconducting state of the cuprates.

There has been debate on whether the μSR results on polycrystalline materials are representative for λ_{ab}, n_s/m^*_{ab} and their changes with p_{sh}.[18,19] The main objections to the validity of the μSR results can be summarized as follows:

While the interpretation of the μSR results in terms of penetration depth and condensate density is based on the existence of a reasonably well-ordered FLL, the strong anisotropy of these materials may give rise to unusual flux states and vortex dynamics. In addition the FLL may be strongly disordered due to pinning on structural imperfections that are caused by dopant atoms, vacancies, twin boundaries, or impurity phases.[17,18] It was even argued that the intrinsic features of the cuprate superconductors can only be observed for optimally doped samples while the results for samples with a reduced transition temperature T_c are dominated by disorder effects.[19]

A further reason for objections was the finding that, for some cuprate systems, the μSR results did not follow such a unique trend. The most prominent examples are the so-called plateau in $YBa_2Cu_3O_{7-\delta}$, where close to $\delta=0$ the depolarization rate σ_0 almost doubles despite a nearly constant transition temperature, and the μSR results on highly anisotropic systems, such as $Bi_2Sr_2CaCu_2O_{8+\delta}$.

The purpose of this paper is to provide a framework in which the behavior of T_c versus σ_0 can now be understood. We summarize our results of TF-μSR and TEP measurements on series of samples that are doped by different sorts and amounts of dopant atoms and that span a wide range of doping. We will show that the magnetic penetration depth $\lambda_{ab}^{-2} \propto n_s/m^*_{ab}$ is determined in a unique way by the hole-doping state of the CuO_2 planes and the consequent critical temperature T_c, and relate the deviations from this universal behavior to specific properties of those systems. For example in Y-123, Y-124, and Y-247 superconductivity is induced in long-range-ordered CuO chains resulting in a substantial contribution to the superconducting condensate density.[8,9,16] Very recent results on the Bi-2212 system show that, due to its extreme anisotropy, the flux state is highly unconventional even at low fields and temperatures, and meaningful values for λ_{ab} indeed cannot be extracted from σ.[18,20]

II. THE TF-μSR METHOD

The μSR experiments were performed at the "surface-muon" beam lines at the Paul-Scherrer Institute (PSI) in Villigen, Switzerland and at TRIUMF in Vancouver, Canada. A detailed discussion of the TF-μSR technique is given in Ref. 11. We give only a brief description of the technique while more emphasis is given to the data analysis.

The samples are field cooled below T_c in an external field (typically $B_{\rm ext}=3$ kG) to induce a homogeneous FLL. Positive muons from a 100% "spin-polarized" muon beam ($p_\mu=29$ MeV/c) are implanted with their initial spin polarization $\vec{P}_\mu(0)$ transverse to $\vec{B}_{\rm ext}$. Without losing their initial spin polarization the muons are rapidly thermalized (10^{-12} s) and come to rest on interstitial lattice sites. They are randomly distributed throughout the field profile of the FLL whose characteristic length scale λ is far larger than any lattice constant. Each muon spin starts to precess around the local magnetic field $B_{\rm loc}$ with a characteristic frequency $\omega_\mu=\gamma_\mu B_{\rm loc}$, where $\gamma_\mu=2\pi\times 135.5$ MHz/T is the gyromagnetic ratio of the muon.

The time-resolved spin polarization $\vec{P}_\mu(t)$ is detected using the parity violation that occurs in muon decay. Each positive muon decays (via the weak interaction) into two neutrinos and a positron, the latter being preferentially emitted in the direction of the muon spin at the instant of decay. The asymmetric position emission rate $N_e^+(t)$ thus contains all the information on the precession and depolarization of $\vec{P}_\mu(t)$.

From a Fourier transform of $\vec{P}_\mu(t)$ one obtains the distribution in the precession frequencies of the muon spins $F(\omega_\mu)$ and, in the case for which the flux lines run parallel to the external field, the field profile of the FLL $\eta(B_{\rm loc})$.[11] For an ideal FLL of an isotropic superconductor the second moments $\langle\Delta\omega_\mu^2\rangle$ and $\langle\Delta B^2\rangle$ are directly related to the magnetic penetration depth λ ($\langle\Delta\omega_\mu^2\rangle \propto \langle\Delta B^2\rangle \propto \lambda^{-2}$). The so-called "line shape" then is highly asymmetric and exhibits characteristic features such as a tail on the high-field side, steps at the maximum and minimum field values, and a pole at the saddle-point value.[21] Such typical features have been observed by TF-μSR measurements on a conventional Nb superconductor[22] as well as on mosaics of $YBa_2Cu_3O_{7-\delta}$ single crystals[23,24] with $B_{\rm ext}$ parallel to the crystal c axis. Slight imperfections of the FLL result in a Gaussian-like smearing of the characteristic sharp features mentioned above.[24]

For polycrystalline samples of the cuprate high-T_c superconductors one only observes a nearly symmetrical and Gaussian shaped distribution $F(\omega_\mu)$, the sharp features are smeared out.[11] For a Gaussian "line shape" the second moment of $F(\omega_\mu)$ may be extracted simply by fitting the μSR-time spectrum by $P_\mu(t) \propto \exp(-\sigma^2t^2/2)$, where the depolarization rate σ is proportional to the second moment of the distribution of the frequencies;

that is $\sigma \propto \langle \Delta\omega_\mu^2 \rangle$.[6-11] The more complicated analysis via the Fourier transformation of $\vec{P}_\mu(t)$ may thus be avoided. Even though the flux lines for these highly anisotropic high-T_c superconductors are, in general, no longer parallel to B_{ext}, the relation

$$\sigma \propto \langle \Delta\omega_\mu^2 \rangle \propto \lambda_{\text{eff}}^{-2} \tag{2}$$

was shown to hold, with $\lambda_{\text{eff}} = 1.23\ \lambda_{ab}$ for $\gamma = \lambda_c/\lambda_{ab} > 5$.[25] Therefore the experimentally determined depolarization rate σ of the muon spin polarization provides a direct measure of the in-plane penetration depth λ_{ab} and hence of the ratio of the superconducting condensate density n_s to the effective mass m_{ab}^* for in-plane motion

$$\sigma[\mu s^{-1}] = 7.086 \times 10^4 \times \lambda_{ab}^{-2}[\text{nm}]$$
$$= 2.51 \times 10^{-21} \times \frac{m_e}{m_{ab}^*} \times n_s[\text{cm}^{-3}]. \tag{3}$$

It has been shown that such a nearly symmetric and Gaussian line shape should be expected in polycrystalline samples due to random orientations of grains of the strongly anisotropic cuprate superconductors and the variation of magnetization in those grains.[26] Then, however, the influences of pinning, unusual flux states, and dynamics cannot be directly estimated (as they can in single-crystal materials) and these generate systematic uncertainties in second moments $\langle \Delta\omega_\mu^2 \rangle$ extracted from μSR on polycrystalline samples. These systematic uncertainties have been the grounds for objections to interpretations of μSR results in terms of λ_{ab} and n_s/m_{ab}^*.[18,19]

These exist, however, quite clear indirect indications of the reliability of the λ_{ab} values as they are derived from the μSR experiments on polycrystalline samples. For example, one finds a reasonable consistency between the low-temperature values of σ_0 and $\lambda_{ab}(0)$ obtained from experiments on polycrystalline or single-crystalline materials.[11,24] In this paper we report on a series of μSR experiments on polycrystalline materials which provide evidence that the low-temperature depolarization rate σ_0 and consequently the penetration depth $\lambda_{ab}(T \rightarrow 0)$ are determined solely by the doping state of the CuO_2 planes p_{sh} and the critical temperature T_c, irrespective of the type and amount of dopant atoms used to achieve p_{sh}. Deviations from this general trend as they occur for some systems can be understood due to their individually different intrinsic properties. For the 123, 124, and 247 systems we show that additional contributions to σ_0 arise from the long-range-ordered CuO chains which act as a second superconducting structural element. We find evidence that the formation of an unusual flux state, even at low temperatures and applied fields, seriously affects the μSR results for σ_0 in the case of the most extremely anisotropic systems only, such as Bi-2212.

The temperature dependence of σ and λ_{ab} as observed for our polycrystalline samples will not be discussed in this paper. This is because a meaningful contribution to this topic can be expected only from experiments on single-crystalline materials, where for example, the effects of thermal fluctuations can be studied. Even though our finding that the CuO chains give an additional contribution to σ and λ_{ab}, which is extremely sensitive on the exact oxygen content and ordering, may provide a key to resolve the, presently, very contradictory experimental results as they are obtained on seemingly identical Y-123 single crystals.

III. SAMPLE PREPARATION AND CHARACTERIZATION

The polycrystalline samples were prepared by standard solid-state reaction methods using high-purity powders. The doping state p_{sh} was determined by measurements of the thermoelectric power (TEP) as described in Refs. 3,7–27. The T_c values were obtained from measurements of the ac susceptibility.

In the case of $Y_{1-x}Ca_xBa_2Cu_3O_{7-\delta}$ we applied a series of sintering steps to avoid a partial substitution of Ca on the Ba site. We mixed stoichiometric amounts of Y_2O_3, $CaCO_3$, $Ba(NO_3)_2$, and CuO (Johnston-Mathey, 99.999%) and decomposed the powders for 1 h at 750 °C in air. Pellets were pressed and sintered at 910 °C in air for 12 h. The sintering temperature was stepwise increased (with intermediate grindings) by 10 °C up to 970 °C. We managed to incorporate large amounts of Ca^{2+} on the Y^{3+} site as is evidenced by the highly overdoped state of the fully oxygenized sample $Y_{0.8}Ca_{0.2}Ba_2Cu_3O_{6.96}$. It has a strongly reduced critical temperature of $T_c = 51$ K and a negative room-temperature TEP value of $S(RT) = -4.5\ \mu V/K$, which is typical for strong overdoping.[3,9]

If the final sintering temperature was too low, energy-dispersive analysis by x rays (EDX) indicated Ba-rich impurity phases and the fully oxidized samples were less overdoped. Sintering at very high temperatures resulted in a Ca-rich impurity phase. To find the phase-pure window between these extremes the sintering temperature was progressively increased with intermediate grinding until Ba-rich phases were eliminated but before Ca-rich phases appeared. Similar treatments combined with low oxygen partial pressure have been successfully used to avoid the occupation of the Ba site by large rare-earth ions.[28]

To achieve full oxygenation we annealed the samples in high-oxygen pressures and lower temperatures than would typically be used for $YBa_2Cu_3O_{7-\delta}$. The samples were heated up to 650 ° in 1 bar O_2 and cooled down to 550 °C within 12 h. Then an oxygen pressure of 60 bar was applied and within 24 h the temperature was ramped down to 350 °C where the samples were kept for several days to one week.

The oxygen contents have been determined by titration measurements, from mass changes, and for both fully oxygenated and optimized samples by neutron diffraction.[29] For higher Ca content the titration results appear to be influenced by small amounts of an impurity phase. As reported in Ref. 30, the titration implies that the maximal achievable oxygen content decreases for higher Ca content. The neutron experiments provide the ability to separate the contributions from impurity phases and to concentrate on the oxygen content of the 1-2-3 phase.

They indicate the same oxygen content of $\delta=0.04(\pm 0.003)$ (Ref. 29) for all the fully oxidized samples with a different Ca content of $x=0.03$, 0.06, 0.1, 0.13, 0.16, and 0.2. The occupation of the "off-chain" O(5) position, however, is found to increase for higher Ca content.

For Y-123 it has been shown that bromination, like full oxygenation, leads to the occurrence of superconductivity with T_c above 90 K.[31] While in the case of full oxygenation the CuO chains are electronically active, they are completely inactivated for the brominated samples.[31] We placed deoxygenated samples of $Y_{1-x}Ca_xBa_{2-y}La_yCu_3O_{6.2}(\delta=0.8)$ in a quartz tube that had a separate reservoir for liquid bromide. The bromine reservoir then was placed in liquid nitrogen in order to freeze out the bromine. This allowed a careful evacuation and sealing of the tube. The Br then was liquified again and the end with the sample was warmed up to 260 °C where it was kept for 30 min. This resulted in a very rapid uptake of Br. The ac susceptibility measurements signaled diamagnetic shielding and T_c values comparable to those of the fully oxidized samples. Longer treatments in the Br atmosphere resulted in reduced shielding and broader transitions. Unfortunately the pellets were heavily cracked by the rapid Br uptake and often crumpled to powder so it was not possible to perform TEP measurements. The Br-doped samples were highly sensitive to exposure to air and had to be stored in sealed containers before they were mounted into the vacuum system of the μSR apparatus.

IV. RESULTS AND DISCUSSION

Before we present and discuss our experimental results we want to refer again to the so-called Uemura plot that summarizes the unique relation between $\sigma_0 \sim n_s(0)/m^*_{ab}$ and $T_c(p_{sh})$ in the underdoped regime. One of the puzzles associated with this plot is the plateaulike deviation from the linear relationship as observed in $YBa_2Cu_2O_{7-\delta}$ for $\delta<0.2$ and its understanding. As we will discuss below, this "plateau" results from a contribution of the charge carriers in the CuO chains to the superconducting condensate density when these CuO chains are sufficiently free of disorder. We will focus first on the results for the underdoped samples before we discuss the optimally to overdoped systems.

A. Underdoped regime

Figure 1 displays our TF-μSR data on a wide set of underdoped samples from various cuprate high-T_c systems. Three different types of systems can be distinguished.

1. Plane only systems

Represented by the full symbols or stars are all samples that exhibit the unique behavior for $\sigma_0 \sim T_c$, following the so-called "Uemura line" (shown by the solid line).[6] While earlier experiments concentrated on "clean" systems like $YBa_2Cu_3O_{7-\delta}$ and $La_{2-x}Sr_xCuO_4$, the samples presented here are as "dirty" as possible with various sorts and amounts of dopant atoms and thus much structural disorder which might affect σ_0. These are $Hg_{0.7}Cr_{0.3}Sr_2CuO_{4+\delta}$ ($T_c=58$ K), $HgBaSrCaCu_{1.8}Re_{0.2}O_{6+\delta}$ ($T_c=91$ K), $La_{1.82}Sr_{0.18}CaCu_2O_{6+\delta}$ ($T_c=48$ K), $Y_{1-x}Ca_xBa_{0.5}Sr_{1.5}Cu_{2.7}Cr_{0.3}O_7$ for $x=0.2$ ($T_c=28$ K) and $x=0.3$ ($T_c=36$ K), strongly deoxygenated $Yb_{0.7}Ca_{0.3}Ba_{1.6}Sr_{0.4}Cu_3O_{7-\delta}$ ($T_c=36$ K and $T_c=58$ K), and $Y_{0.8}Ca_{0.2}Ba_2Cu_3O_{7-\delta}$ ($T_c=51$ K) as well as fully oxygenated $NdBa_2Cu_3O_{7-\delta}$ ($T_c=94$ K). It is obvious that the degree of disorder due to the different substitutions does not quantitatively affect the μSR data. All these very different samples have two features in common. First, they do not contain fully oxygenated or long-range-ordered CuO chains that may give rise to an addi-

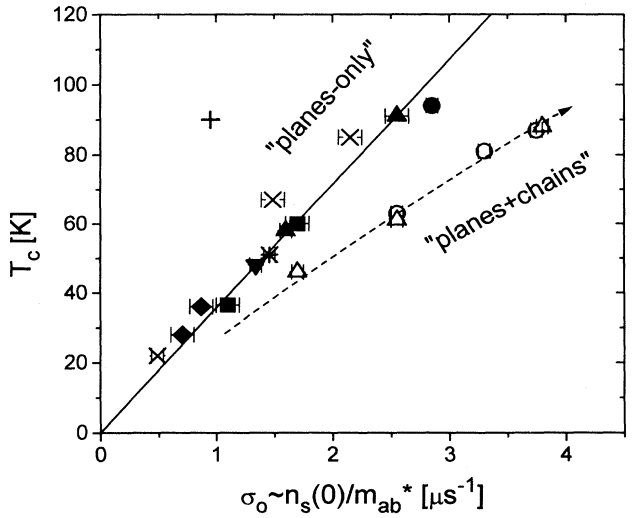

FIG. 1. T_c plotted as a function of the low-temperature μSR depolarization rate σ_0 for various samples from the underdoped regime. The solid line represents the so-called "Uemura line" for underdoped plane-only samples (Ref. 6). Shown by solid symbols are our results on several highly nonstoichiometric underdoped samples; (solid triangles) $Hg_{0.7}Cr_{0.3}Sr_2Cu_{4+\delta}$ ($T_c=58$ K) and $HgBaSrCaCu_{1.8}Re_{0.2}O_{6+\delta}$ ($T_c=91$ K), (solid inverted triangles) $La_{1.82}Ca_{1.18}Cu_2O_{6+\delta}$ ($T_c=48$ K), (solid diamonds) $Y_{1-x}Ca_xBa_{0.5}Sr_{1.5}Cu_{2.8}Cr_{0.2}O_7$ for $x=0.2$ and 0.3 ($T_c=28$ and 36 K), (solid squares) strongly deoxygenated $Yb_{0.7}Ca_{0.3}Ba_{1.6}Sr_{0.4}Cu_3O_{7-\delta}$ ($T_c=36$ and 58 K), (solid star) $Y_{0.8}Ca_{0.2}Ba_2Cu_3O_{7-\delta}$ ($T_c=51$ K), and (solid circle) fully oxygenated $NdBa_2Cu_3O_{7-\delta}$ ($T_c=94$ K). The plus symbol + which lies far off the universal line for plane-only samples, represents a typical result for an optimally doped sample of the extremely anisotropic system $Bi_2Sr_2CaCuO_{8+\delta}$. Indicated by the × are our results for the slightly less anisotropic, underdoped samples of $Bi_{1.7}Pb_{0.3}Sr_{2-x}La_xCa_{0.9}CuO_{8+\delta}$ with $T_c=22$, 61, and 85 K. The results for underdoped samples with long-range-ordered CuO chains (plane + chain samples) follow a separate line (dashed line). They are shown by (open circles) for $YBa_2Cu_4O_8$ ($T_c=81$ K), $Y_{0.9}Ca_{0.1}Ba_2Cu_4O_8$ ($T_c=87.5$ K), and $YBa_{1.85}La_{0.15}Cu_4O_8$ ($T_c=63$ K) and by open triangles for $Y_2Ba_4Cu_7O_{15-\delta}$ ($T_c=90$, 63, and 46 K).

tional contribution to σ_0 and n_s/m^*_{ab}. Second, all of them are more isotropic than the very anisotropic system, Bi-2212.

The CuO chains of the underdoped $Yb_{0.7}Ca_{0.3}Ba_{1.6}Sr_{0.4}Cu_3O_{7-\delta}$ and $Y_{0.8}Ca_{0.2}Ba_2Cu_3O_{7-\delta}$ are strongly deoxygenated ($\delta > 0.5$). For fully oxygenated $Y_{1-x}Ca_{0.3}Ba_{0.5}Sr_{1.5}Cu_{2.7}Cr_{0.3}O_{7-\delta}$ the long-range order of the CuO chains is effectively interrupted by the Cr substituents that are incorporated on the Cu(1) chain sites.[32] In the case of fully oxygenated $NdBa_2Cu_3O_{7-\delta}$, Cu-NQR-measurements show that the long-range order in the CuO chains is by far less developed than for comparably oxygenated samples with other rare earths like Y, Gd, or Tm.[33]

2. *Systems containing both planes and chains*

Indicated in Fig. 1 by the open symbols are all the underdoped samples that contain fully oxygenated and long-range ordered CuO chains such as $YBa_2Cu_4O_8$, $Y_{0.9}Ca_{0.1}Ba_2Cu_4O_8$, $YBa_{1.85}La_{0.15}Cu_4O_8$, and $Y_2Ba_4Cu_7O_{15-\delta}$. As reported earlier,[8,34] all of them exhibit enhanced values of $\sigma_0 \sim n_s/m^*_{ab}$ when compared with the "Uemura line" for "plane-only" samples. They form a separate straight line for "plane+chain" samples that is indicated by the dashed line. Again one can see that the changes in σ_0 are determined solely by the corresponding changes in p_{pl} and T_c, while the concentration of the dopant atoms is irrelevant. $Y_{0.9}Ca_{0.1}Ba_2Cu_4O_8$ ($T_c = 87$ K) and $YBa_{1.85}La_{0.15}Cu_4O_8$ ($T_c = 63$ K) contain similar amounts of dopant atoms, however, T_c and p_{pl} are increased if Ca^{2+} is substituted for Y^{3+}, whereas they decrease if Ba^{2+} is replaced by La^{3+}. The data point for the unsubstituted sample resides on the line between these two samples.

3. *Systems with large anisotropy*

The + symbol in Fig. 1 is representative of the μSR results on nearly optimally doped samples of the extremely anisotropic system $Bi_2Sr_2CaCu_2O_{8+\delta}$, the crosses ($\times$) in the same figure show underdoped samples of the (due to Pb doping) slightly less anisotropic system $Bi_{1.7}Pb_{0.3}Sr_{2-x}La_xCa_{0.9}Cu_2O_{8+\delta}$.[35] The σ_0 value for $Bi_2Sr_2CaCu_2O_{8+\delta}$ is very low and deviates clearly from the general trend observed for the other less anisotropic systems. For the somewhat less anisotropic $Bi_{1.7}Pb_{0.3}Sr_{2-x}La_xCa_{0.9}Cu_2O_{8+\delta}$, however, the σ_0 values come already very close to the Uemura line. A key for the understanding of this phenomenon may be found from the results of very recent experiments on single-crystalline $Bi_2Sr_2CaCu_2O_{8+\delta}$, which indicate a sudden reduction in the dimensionality of the vortex system when the external field exceeds a critical field B_{cr}.[18,20,38] A structure of extended flux lines, which is one of the basic assumptions for the interpretation of the μSR depolarization rate σ in terms of λ_{ab}, is observed only for fields lower than the critical field $B_{c_1} < B_{ext} < B^* \approx 500G$.[20] At B^* the flux structure exhibits a clear change which is best described as an array of so-called "pancake vortices" which are uncorrelated between different blocks of superconducting CuO_2 (bi,tri) layers but ordered independently within each layer.

It has been shown by magnetization experiments[37] and just recently by μSR experiments[38] that B^* depends essentially on the anisotropy of the system. For strongly overdoped and less anisotropic $Bi_2Sr_2CaCu_2O_{8+\delta}$ it was shown that B_{cr} increases rapidly to values of more than 1 kG.[37,38] Whereas B^* is found to fall below 100 G in strongly underdoped and highly anisotropic samples.[38] Magnetization measurements of B^* on different Tl systems also indicate that B^* depends essentially on the thickness of the nonsuperconducting blocking layers.[39]

While the applied field has to be significantly lower than B^* so that the assumption of an extended FLL is justified, a strong overlap of the vortices [corresponding to $B_{ext} \sim 1$ kG] is required to order that meaningful values of λ_{ab} can be extracted from the depolarization rate.[11,21] It seems that both of these contradictory requirements can no more be fulfilled in the case of the extremely anisotropic underdoped and optimally doped $Bi_2Sr_2CaCu_2O_{8+\delta}$ and the σ_0 values are no more related to the penetration depth λ_{ab} in the usual way. In the case of the less anisotropic lead-doped samples $Bi_{1.7}Pb_{0.3}Sr_{2-x}La_xCa_{0.9}Cu_2O_{8+\delta}$, however, it seems that B^* is sufficiently enhanced that the σ_0 values follow the otherwise universal trend, and may be interpreted in terms of $\lambda_{ab}(T \to 0)$ as for the other less anisotropic systems (see Sec. IV A 1).

As far as we know there is only one more case for which the μSR data do not follow the unique trend $\sigma_0 \sim n_s/m^*_{ab} \sim T_c$, namely, incorporation of dopant atoms like Zn or Ni directly into the CuO_2 planes.[40] In this case it has been shown that T_c is not suppressed by a reduction of p_{sh} but due to a different mechanism that is presently not fully understood.[3] Consequently, $\sigma_0 \sim n_s/m^*_{ab}$ is not expected to correlate with T_c in the usual way.

Summarizing the results for the underdoped regime we find that the relation $\sigma_0 \propto \lambda(0)^{-2}_{ab} \propto n(0)_s/m^*_{ab} \propto T_c$ is a unique feature of all underdoped "plane-only" systems. The μSR results for σ_0 are not sensitive on disorder caused by dopant atoms or vacancies, and except for the most anisotropic system Bi-2212, the μSR results for σ_0 do not seem to depend strongly on the anisotropy. Enhanced condensate densities are observed for systems that contain fully oxygenated and well-ordered CuO chains.

B. Optimally to overdoped regime

Our data for optimally and overdoped "plane-only" samples are shown in Fig. 2 by crosses ($\times$) for $Tl_2Ba_2CuO_{6+\delta}$ and by stars for $Y_{1-x}Ca_xBa_2Cu_3O_{6.2}Br_z$ for $x = 0$ ($T_c = 92$ K) and $x = 0.2$ ($T_c = 49$ K). The solid lines indicate the typical evolution of σ_0 for "plane-only" samples of the systems Tl-2201 and Y-123, the arrows point towards an increasing p_{sh}. The most prominent feature is the strong reduction of $\sigma_0 \sim n_s/m^*_{ab} \sim T_c$ in the heavily overdoped regime, in spite of an increased hole

concentration p_{sh}.[7,10] We have interpreted this behavior in terms of pair-breaking effects that become dominant with overdoping and thus suppress both T_c and the condensate density n_s.[7] Other interpretations have been suggested[10,41,42] but a consensus interpretation of this phenomenon is still lacking.

Also shown in Fig. 2 by solid and open symbols are our data for optimally to overdoped samples of $Y_{1-x}Ca_xBa_2O_{7-\delta}$ with the open circles in case of $x=0$, solid circles for $x=0.03$, open triangles for $x=0.06$, solid triangles for $x=0.13$, open squares for $x=0.2$, and solid squares for $Yb_{0.7}Ca_{0.3}Ba_{1.6}Sr_{0.4}Cu_3O_{7-\delta}$. All these samples contain CuO chains which provide an additional contribution to the condensate density (besides that of the CuO_2 planes), once they are nearly fully oxygenated ("plain+chain samples"). For these samples p_{sh} is increased by Ca doping as well as by the oxygenation of the CuO chains. With higher Ca content the fully oxygenated samples are, therefore, more heavily overdoped. A deoxygenation of the CuO chains results in an increase of T_c up to the maximum $T_{c,\max}$ before T_c is decreased again in the underdoped regime.[9,27,30] This enabled us to study a series of samples with different Ca content, but each with an optimized doping state p_{sh} in the CuO_2 planes (as confirmed by TEP measurements) and, therefore, with a different degree of chain filling.

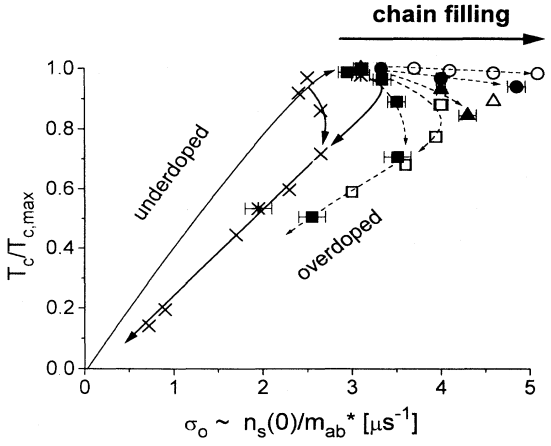

FIG. 2. $T_c/T_{c,\max}$ plotted as a function of the low-temperature depolarization rate σ_0 for the optimally to heavily overdoped regime. The typical "boomerang" shaped paths for the plane-only systems are indicated by the solid lines, the arrows point towards increasing doping, p_{sh}. Data points are shown by crosses ($\times$) for $Tl_2Ba_2CuO_{6+\delta}$ and by solid stars for $Y_{1-x}Ca_xBa_2Cu_3O_{6.2}Br_z$ for $x=0$ and 0.2 ($T_c=92$, 49 K) that have electronically inactive CuO chains (Ref. 31). The samples with electronically active planes and chains are shown by (open circles) $Y_{1-x}Ca_xBa_2Cu_3O_{7-\delta}$ for $x=0$ and $0.02<\delta<0.12$, (solid circles) $x=0.03$ and $0.04<\delta<0.175$, (open triangle) $x=0.06$ and $\delta=0.04$, (solid triangle) $x=0.13$ and $0.06<\delta<0.27$, (open square) $x=0.20$ and $0.04<\delta<0.38$, and (solid square) for $Yb_{0.7}Ca_{0.3}Ba_{1.6}Sr_{0.4}Cu_3O_{7-\delta}$. The dashed lines and the arrows point towards an increasing oxygen content and p_{sh}.

The samples with fully oxygenated CuO chains ($\delta<0.25$) have significantly higher σ_0 values than the corresponding "plane-only" samples. The differences between "plane-only" and "plane+chain" samples are clearly related to the final filling of the CuO chains. This effect becomes obvious in the so-called "90 K plateau" in σ_0 versus T_c for $YBa_2Cu_3O_{7-\delta}$ with $\delta<0.2$.[43] Here the final filling of the chains nearly coincides with optimum doping, where the changes in T_c are small. This "plateau" in σ_0 versus T_c around optimum doping disappears gradually with higher Ca content x and is completely absent for $x=0.2$ and $x=0.3$ where the additional chain condensate is expected to appear only in the heavily overdoped regime.[9,16] This so-called "90 K plateau" in σ_0 versus T_c was regarded as a clear indication for an "ill-defined" relationship of the μSR-depolarization rate σ_0 to λ and n_s/m_{ab}^*.[18] Our data, however, show that the additional contribution to $\sigma_0 \sim n_s/m_{ab}^*$ is caused by the superconducting condensate in sufficiently long-range-ordered, metallic CuO chains.[8,9,16]

The metallic character of the CuO chains is evidenced by short nuclear quadrupole resonance (NQR) relaxation times,[44] field-dependent heat capacity,[45] infrared conductivity and reflectivity,[46,47] electron energy loss spectroscopy (EELS),[48] TEP[49,3] and other dc transport properties.[50] A pronounced anisotropy due to the CuO chains has been predicted by band calculations.[51] The proximity of these metallic chains to the intrinsically superconducting CuO_2 planes causes induced superconductivity on the chains[52] and an accompanying enhancement in the total condensate density as the carriers in the chains condensate into Cooper pairs.

The superconducting condensate in the CuO chains has been identified only recently,[8,9,16,52] probably because it is so rapidly suppressed by any sort of disorder in the CuO chains. The consequent anisotropy between λ_a and λ_b has been observed lately by microwave and far infrared measurements on detwinned crystals of fully oxygenated Y-123 and Y-124 (Ref. 53) and has also been inferred from μSR studies.[16] Very recent measurements of the jump of the specific on well oxygenated Y-123 single crystals show that the final filling of the CuO chains is accompanied by an increase of the condensation energy.[54] For a fully oxidized and therefore slightly overdoped crystal with a reduced T_c value the condensation energy is clearly higher than for a less fully oxidized but optimally doped sample with $T_c=T_{c,\max}$.[54]

It is interesting to note that the additional chain condensate does not have a significant influence on the critical temperature T_c. This may be seen already from the "90 K plateau" of $YBa_2Cu_3O_{7-\delta}$ where the condensate density is drastically increased when the CuO chains are completely filled, while T_c is hardly changed. In Fig. 3 we show the values of $T_{c,\max}$ for several optimized series in the system $Y_{1-x}Ca_xBa_2Cu_{3-y}Co_yO_{7-\delta}$. All these samples have the same optimal carrier concentration in the CuO_2 planes as confirmed by TEP measurements and the higher their Ca content, the more oxygen deficient

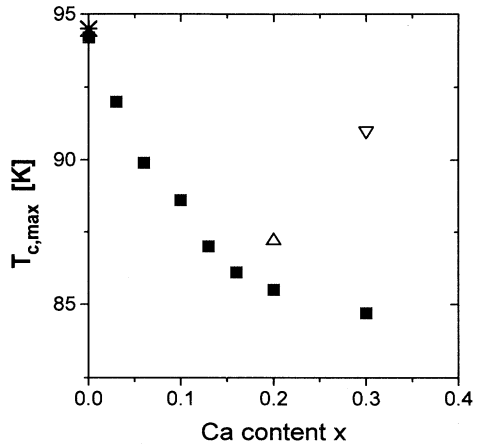

FIG. 3. The optimal critical temperature $T_{c,\max}$ of the systems $Y_{1-x}Ca_xBa_2Cu_{3-y}Co_yO_{7-\delta}$ for variable oxygen content plotted versus the Ca content. The data are shown by (solid squares) for $x=0$, 0.03, 0.06, 0.13, 0.16, 0.20, 0.30, and $y=0$, (open triangle) for $x=0.20$ and $y=0.05$, (open invertex triangle) for $x=0.30$ and $y=0.20$. With increasing Ca and Co content the CuO chains of these optimized samples are more disordered and electronically less active. Shown by a star is $T_{c,\max}$ for $YBa_{1.95}La_{0.05}Cu_3O_{6.2}Br_z$, a sample that has completely inactive CuO chains (Ref. 31) but $T_c=94.5$ K.

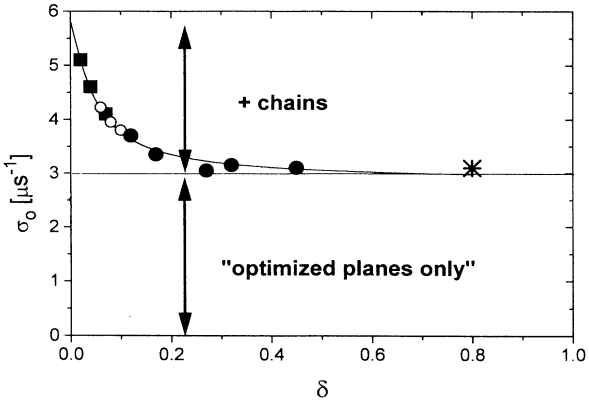

FIG. 4. The low-temperature depolarization rate σ_0 for optimally doped $Y_{1-x}Ca_xBa_2Cu_3O_{7-\delta}$ plotted as a function of the oxygen deficiency, δ. Solid squares indicate slightly overdoped $YBa_2Cu_3O_{7-\delta}$ for $\delta=0.02$, 0.04, and 0.07 (Ref. 43), solid circles optimized samples for $x=0$, 0.03, 0.06, 0.13, and 0.20 and (solid star) $YBa_2Cu_3O_{6.2}Br_z$ with $T_c=92$ K. The solid line shows the fit by Eq. (4) with $\sigma^{pl}=2.95\ \mu s^{-1}$, $\sigma^{ch}(\delta\to 0)=8.1\ \mu s^{-1}$ [$\lambda_a=155$ nm and $\lambda_b(\delta\to 0)=80$ nm], and $\xi^{ch}=5.6$ nm.

and disordered are their CuO chains. The additional doping of Co on the Cu(1) chain site leads to an even stronger, direct disruption of the ordering of the CuO chains. Even though $T_{c,\max}$ is slightly reduced by the Ca doping, from 94 K for $x=0$ to 85.5 K for $x=0.2$ (as shown by the solid squares), it is increased again with the additional doping of Co (open symbols). For a sample $YBa_{1.95}La_{0.05}Cu_3O_{6.2}Br_z$, that has completely inactive CuO chains,[31] the critical temperature is as high as $T_c=94.5$ K (shown by the star). This shows that the ordering of the CuO chains and the consequent formation of a superconducting condensate in the chains does not have a pronounced effect on the values of $T_{c,\max}$.

1. Analysis of the chain condensation

The evolution of the chain condensate with the depletion of the CuO chains is displayed in Fig. 4. The values of σ_0 and δ are shown for the samples with (nearly) optimized CuO_2 planes ($T_c\sim T_{c,\max}$) but successively depleted CuO chains. The solid squares indicate slightly overdoped $YBa_2Cu_3O_{7-\delta}$ with $\delta=0.02$, 0.04, and 0.07,[11,55] the solid circles represent optimally doped $Y_{1-x}Ca_xBa_2Cu_3O_{7-\delta}$ with ($x=0$, $\delta=0.13$), ($x=0.03$, $\delta=0.175$), ($x=0.06$, $\delta=0.21$), ($x=0.13$, $\delta=0.27$), and ($x=0.2$, $\delta=0.38$). The brominated sample $YBa_2Cu_3O_{6.2}Br$ ($\delta=0.8$) which has inactive CuO chains[31] is shown by a star. The open circles represent the results for $TmBa_2Cu_3O_{7-\delta}$ (see discussion below). With increasing δ the σ_0 values first drop sharply before they saturate for $\delta>0.20$. The saturation value of around 3.0(1) μs^{-1} represents the typical contribution only from the optimally doped CuO_2 planes. Again it becomes obvious that the chain condensate does not appear until the CuO chains are sufficiently long-range-ordered and free of disorder by oxygen vacancies.

All our experiments have been performed on polycrystalline samples where the μSR depolarization rate measures only an effective penetration depth $\sigma_0\propto\lambda(0)_{\rm eff}^{-2}$. An exact theory has been worked out only for systems with uniaxial anisotropy[25] where $\lambda_{\rm eff}=1.23\ \lambda_{ab}$ for $\gamma=\lambda_c/\lambda_{ab}>0.5$. Taking the in-plane anisotropy into account a reasonable approximation should be given by $\lambda_{\rm eff}=1.23\sqrt{\lambda_a\lambda_b}$.

Our data are well described by a simple model (see solid line in Fig. 4). We assume that the condensate in the chains contributes only to the shielding currents along the direction of the chains. The measured depolarization rate $\sigma_{\rm eff}$ then is the geometric mean of the components parallel and transverse to the CuO chains $\sigma^{\rm eff}=\sqrt{\sigma^{pl}(\sigma^{pl}+\sigma^{ch})}$ with $\sigma^{pl}\propto n_s^{pl}/m_{ab}^{pl}$ and $\sigma^{ch}\propto n_s^{ch}/m_{ab}^{ch}$. Further, the oxygen vacancies are assumed to be randomly distributed throughout the CuO chains and to act as scattering centers which results in the scattering length $l^{ch}=b/\delta$. Within a Drude-model, the reduction in σ^{ch} due to such scattering is determined by the factor $(2/\pi)\tan^{-1}(2b/\pi\xi_0^{ch})$. Since p_{sh} appears to vary linearly with δ over a fairly wide range,[56] the concentration of chain carriers should be reduced by a factor of $1-\delta$ yielding the result:

$$\sigma_{\rm eff}^2=\sigma^{pl}[\sigma^{pl}+\sigma^{ch}(1-\delta)\tan^{-1}(2b/\pi\xi_0^{ch}\delta)]\ . \qquad (4)$$

Assuming $\sigma_0^{pl}=2.95\ \mu s^{-1}$ as is indicated in Fig. 4 by the saturation of σ_0 for increasing δ, we obtain a reasonable fit as shown by the solid line. The fitted parameters

are $\sigma_0^{ch}=8.1\ \mu s^{-1}$ and $\xi_0^{ch}=5.6$ nm. The resulting in-plane penetration depth exhibits for $\delta\rightarrow 0$ a pronounced anisotropy with $\lambda_a=155$ nm and $\lambda_b(\delta\rightarrow 0)=80$ nm which is in good agreement with recent results from microwave measurements.[53] By assuming that for $\delta\rightarrow 0$ all mobile carriers in both the nearly optimally doped CuO_2 planes and in the CuO chains participate in the superconducting condensate, we derive

$$\frac{\sigma_0^{ch}}{\sigma_0^{pl}}=\frac{m_{pl}^*}{m_{ch}^*}\frac{1-2p_{pl}}{2p_{pl}}\ , \tag{5}$$

where we have taken $n_s^{pl}\propto 2p_{sh}$ and $n_s^{ch}\propto p_{ch}=1-2p_{sh}$. Assuming $p_{sh}=0.16$ holes per CuO_2 plane in the unit cell[1] we find a mass ratio of $m^{pl}/m^{ch}\approx 4/3$ which is in good agreement with the experimental and theoretical predictions.[48]

2. *Comparison with the results from neutron diffraction and Cu-NQR*

The suppression of the chain-condensate was described above by a simplified model, in which the oxygen vacancies are randomly distributed. The ordering of the oxygen atoms and vacancies, however, is likely to be more complicated. The oxygen may partially occupy the interchain O(5) position or the oxygen vacancies may form clusters. Techniques like neutron scattering or Cu-NQR provide additional information on the structural ordering of the CuO chains that can be compared with our μSR results for the chain condensate.

Neutron scattering experiments indicate the same oxygen content of $\delta=0.04$ for our fully loaded samples with different Ca content.[29] For the samples with higher Ca content, however, the occupancy of the interchain O(5) position is found to be more pronounced. In Fig. 5 we show the additional chain contribution to the depolarization rate σ^{ch} by the same symbols used in Fig. 2. According to Eq. 4 we assumed $\sigma^{ch}=\sigma_0^2/\sigma^{pl}-\sigma^{pl}$, where σ^{pl} was estimated from the solid line in Fig. 2 for optimally to overdoped "plane-only" 123 samples. Obviously, the maximal chain condensate is reduced for higher Ca content. This reduction parallels the increase of the O(5) occupancy (see Table I) and demonstrates that the density of the chain condensate is not only determined by the overall oxygen content but also by the degree of long-range order within the CuO chains.

Cu-NQR experiments provide an interesting possibility to check the local arrangement of the oxygen in the CuO chains.[33] Due to the different electric field gradients at Cu(1) sites with two, three, or four oxygen neighbors one can derive an average length n of the ordered CuO chain fragments. Lütgemeier *et al.* observe that the oxygen vacancies in (Y, Gd, Tm)-123 tend to cluster, so that empty and filled chain fragments are formed.[33] For $0.3<\delta<0.5$ the ordered chain fragments extend only over around 10 unit cells ($n<10$). For $\delta<0.3$ a very rapid growth in n is observed, but for $\delta<0.15$ and $n>50$ it is difficult to estimate the mean length of the ordered chain fragments because of the few Cu(1) sites with twofold or threefold oxygen coordination. For a direct comparison of the Cu-NQR values for n (Ref. 33) with our μSR results for σ^{ch} we must have correct absolute values of δ, but the conventions for the absolute oxygen contents δ are likely to be different. We performed TF-μSR experiments on three of the samples used for the NQR experiments. From their position on the solid line in Fig. 4 (shown by open circles) we estimate the δ values according to our convention (shown in Table II). We find good agreement for the relative differences in the δ values, but the absolute δ values are found to be higher than those reported by Lütgemeier *et al.*[33] by 0.06

Using this adjustment for δ the average lengths of the chain fragments n can be compared with our results for

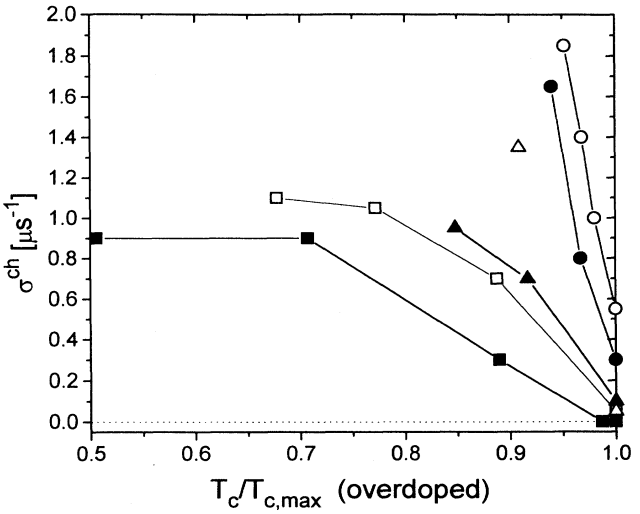

FIG. 5. The chain contribution to the μSR depolarization rate σ^{ch} plotted as a function of $T_c/T_{c,max}$ for optimally and overdoped "plane + chain" samples. As indicated by Eq. (4) we assumed $\sigma^{ch}=\sigma_0^2/\sigma^{pl}-\sigma^{pl}$. Shown by the same symbols in Fig. 2 are the corresponding σ_0 values. The values for σ^{pl} are taken from the "boomerang path" (solid line) in Fig. 2 as it is estimated for "plane-only" Y-123.

TABLE I. Shown for $Y_{1-x}Ca_xBa_2Cu_3O_{7-\delta}$ are the Ca content x, oxygen deficiency δ, occupation of the interchain O(5) position, occupation of the in-chain O(1) position, and the μSR-results for the chain contribution to the depolarization rate σ^{ch}. The chain contribution σ^{ch} is reduced by an increased oxygen deficiency δ as well as by a higher occupation of the interchain O(5) position that occurs for higher Ca content.

Ca content	δ	O(5) occupation	O(1) occupation	σ^{ch} [μs^{-1}]
0	0.07(1)	0.03(1)	0.90(1)	2.5(2)
0.03	0.04(1)	0.034(1)	0.928(1)	4.3(2)
0.06	0.04(1)	0.045(1)	0.915(1)	3.4(2)
0.10	0.04(1)	0.053(1)	0.907(1)	
0.13	0.06(1)	0.053(1)	0.889(1)	2.5(2)
0.20	0.04(12)	0.052(1)	0.907(1)	2.7(2)

TABLE II. The oxygen deficiency δ and Cu-NQR results for the average length n of ordered chain fragments (Ref. 33) for (Y,Cd,Im)-123 in comparison with the μSR results for the chain contribution σ^{ch}. The first three samples have been investigated by both the μSR (open circles in Fig. 6) and Cu-NQR (Ref. 33). For the others σ^{ch} was estimated from the μSR-results on comparable samples shown in Fig. 6. A correlation between the chain contribution and the length n of the ordered chain fragments can be seen.

δ	n	σ^{ch} [μs^{-1}]
0.06	> 50	2.9(2)
0.08	> 50	2.2(2)
0.10	> 50	1.8(2)
0.20	50	0.7(2)
0.25	30	0.5(2)
0.30	13	0.3(2)
0.40	9	0.2(2)

σ^{ch} (see Table II). In spite of the crude assumptions, the rapid growth of n for $\delta < 0.30$ is clearly correlated with the appearance of a large chain condensate σ^{ch}. A lower limit for ξ^{ch} is given by the finding that the chain condensate is absent for $n < n^{\min} \sim 10$, which implies $\xi^{ch} > 3.8$ nm.

The Cu-NQR experiments on $NdBa_2Cu_3O_{7-\delta}$ imply comparably very short lengths of the ordered chain fragments, even when δ is small.[33] We have performed a TF-μSR measurement on such a fully loaded sample. The result was already shown in Fig. 1 and it exhibits a σ_0 value only slightly higher than expected for a "plane-only" system. Also shown in Fig. 1 are the results for fully oxygenated $Y_{1-x}Ca_xBa_{0.5}Sr_{1.5}Cu_{2.8}Cr_{0.2}O_7$ which indicate that not only oxygen vacancies but also other disruptions of the long-range ordering in the CuO chains destroys the chain condensate.

Even though $YBa_2Cu_4O_8$ and $Y_2Ba_4Cu_7O_{15-\delta}$ contain long-range-ordered chains, our μSR results indicate that the chain condensate is not as well developed as for fully oxygenated $YBa_2Cu_3O_{6.98}$. The total depolarization rate for $YBa_2Cu_4O_8$ is $\sigma_0 = 3.25\ \mu s^{-1}$, whereas the typical value for such a "plane-only" system with underdoped CuO_2 planes ($T_c = 80$ K) is about $\sigma^{pl} = 2.25\ \mu s^{-1}$. From this we derived $\sigma^{ch} = 2.44\ \mu s^{-1}$. For the less underdoped system $Y_{0.9}Ca_{0.1}Ba_2Cu_4O_8$ ($T_c = 87$ K) the total depolarization rate is $\sigma_0 = 3.75\ \mu s^{-1}$ and $\sigma^{pl} = 2.45\ \mu s^{-1}$, thus $\sigma^{ch} = 3.3\ \mu s^{-1}$. For the more underdoped sample $YBa_{1.85}La_{0.15}Cu_4O_8$ ($T_c = 63$ K) we obtain $\sigma_0 = 2.55\ \mu s^{-1}$ and $\sigma^{pl} = 1.75\ \mu s^{-1}$ which results in $\sigma^{ch} = 1.93\ \mu s^{-1}$. These results have to be compared with the values of $\sigma^{ch} = 5.3\ \mu s^{-1}$ for $YBa_2Cu_3O_{6.98}$ or even with $\sigma^{ch} = 8.1\ \mu s^{-1}$ when $\delta = 0$ as is indicated by the fit. The number of mobile carriers per double CuO chain in the 124 structure should be at least as high as in a fully oxygenated single chain of the 123 system. This discrepancy in the densities of the chain condensate suggests that only parts of the carriers in the double CuO chains of underdoped 124 contribute to the superconducting condensate. A less effective proximity coupling between the intrinsically superconducting CuO_2 planes and the intrinsically normal conducting CuO chains may be caused either by the underdoped state of the CuO_2 planes or by the wider spacing of the CuO_2 bilayers due to the double CuO chains. Further experiments on $YBa_{1-y}La_yCu_3O_7$ may help to resolve this problem.

In conclusion, we find that our μSR experiments demonstrate the existence of a superconducting condensate in the CuO chains. At present, however, they provide only some trends and ideas towards the mechanisms of its development or suppression.

V. SUMMARY

TF-μSR and TEP experiments on polycrystalline high-T_c cuprate superconductors provide clear evidence that $\sigma_0 \propto \lambda(0)_{ab}^{-2} \propto n_s(0)/m_{ab}^*$ is determined in a unique way by the critical temperature T_c and the doping state p_{sh} of the CuO_2 planes. The generic phase diagram is sketched in Fig. 6. The solid lines are representative of systems where the CuO_2 planes are the only structural element that contributes to the superconducting condensate

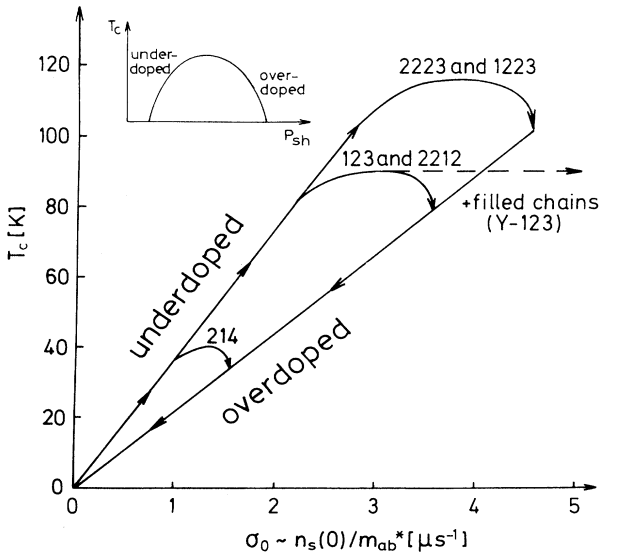

FIG. 6. A sketch of the unique relationship between the low-temperature depolarization rate $\sigma_0 \propto n_s(0)/m_{ab}{}^*$ and the critical temperature T_c. The solid lines represent the "boomerang" shaped paths as they are typically observed for the different plane-only systems. The arrows point towards increasing doping, p_{sh}. The underdoped and the overdoped regime are characterized each by a linear relation $\sigma_0 \propto n_s(0)/m_{ab}^* \propto T_c$. The maximal critical temperature $T_{c,\max}$ of a system determines the maximum value of σ_0. The "90 K plateau" in $YBa_2Cu_3O_{7-\delta}$ for $\delta < 0.25$ (shown by the dashed line) arises due to the additional condensation of the carriers in the long-range ordered CuO chains (plane+chain samples). The inset shows the typical dependence of the critical temperature T_c on the doping state of the CuO_2 sheets, p_{sh}.

("plane-only" samples). The arrows point in the direction of an increasing carrier concentration p_{sh}. Disorder effects caused by dopant atoms have no significant influence on the μSR-depolarization rate σ_0.

The dashed line indicates the so-called "plateau" in σ_0 versus T_c as observed in $YBa_2Cu_3O_{7-\delta}$ for $\delta < 0.2$. We have argued that the increase of σ_0 is due to a contribution of the charge carriers in sufficiently long-range-ordered CuO chains to the superconducting condensate density. The additional chain condensate also causes enlarged σ_0 values in underdoped Y-124 and Y-247. The critical temperature T_c is hardly affected by the formation of the chain condensate but seems to be determined by the intrinsic properties of the CuO_2 planes. This implies that the condensation of the chain carriers is induced by proximity and charge transfer effects with the neighboring, intrinsically superconducting CuO_2 planes.[52] Slightest amounts of disorder in the CuO chains lead to a very rapid suppression of the chain condensate. This extreme sensitivity on disorder accounts for the wide spread in reported values for the (temperature dependence of the) condensate density, condensate energy, in-plane anisotropy, interlayer coupling, and flux pinning deduced from measurements on apparently nearly identical samples in the "90 K plateau" of Y-123. This emphasizes the need for very accurate characterization of the oxygen nonstoichiometry and oxygen disorder in oxygenated 123, especially in the case of single crystals which are difficult and slow to load with oxygen.

Analysis of our data by a model in which the additional chain condensate is mobile just along the chain direction and suppressed by scattering on randomly distributed oxygen vacancies yields a chain coherence length of $\xi_0^{ch} \cong 5.6$ nm and a pronounced in-plane anisotropy for optimized Y-123 with $\lambda_a = 150$ nm and $\lambda_b(\delta \to 0) = 80$ nm.

We compared our μSR data for the chain condensate with the results from neutron scattering[29] and Cu-NQR experiments[33] that provide more information on the oxygen ordering in the chains. For higher Ca content the occupation of the O(5) interchain position is enhanced, and the chain condensate is correspondingly reduced. In (Y,Gd,Tm)-123 the oxygen vacancies form clusters, supporting the formation of long-range-ordered chain fragments and, consequently, of a large chain condensate. In Nd-123, however, the oxygen vacancies are randomly distributed, the chain fragments are significantly shorter and the chain condensate is strongly suppressed.

In highly anisotropic cuprate systems, such as $Bi_2Sr_2CaCu_2O_{8+\delta}$, an unconventional flux state is formed even at the lowest temperatures. Therefore, the μSR results for σ_0 do not follow the unique trend and cannot be interpreted in terms of λ_{ab} and n_s/m^*_{ab}. Already for the slightly less anisotropic system $Bi_{1.7}Pb_{0.3}Sr_{2-x}La_xCa_{0.9}Cu_2O_{8+\delta}$, however, the unique trend is almost recovered.

ACKNOWLEDGMENTS

We would like to thank H. Lütgemeir, K. Kishio, and C. Greaves for providing some of the samples. We would also like to thank D. Herlach (PSI), C. Ballard (TRIUMF), and S. Kreitzman (TRIUMF) for the technical support during the μSR experiments. This work was supported by the BMFT. One of us (C.B.) gratefully acknowledges the financial support by the DAAD (Deutscher Akademischer Austauschdienst).

[1] J. L. Tallon, R. G. Buckley, E. M. Haines, M. R. Presland, A. Mawdsley, N. E. Flower, and J. Loram, Physica C **185-189**, 855 (1991); H. Zhang and H. Sato, Phys. Rev. Lett. **70**, 1697 (1993).

[2] H. Takagi, B. Batlogg, H. L. Kao, R. J. Cava, J. J. Krajewski, and W. F. Peck, Jr., Phys. Rev. Lett. **69**, 2975 (1992).

[3] S. D. Obertelli, J. R. Cooper, and J. L. Tallon, Phys. Rev. B **46**, 14 928 (1992).

[4] T. Nishikawa, J. Takeda, and M. Sato, J. Phys. Soc. Jpn. **62**, 2568 (1993); H. Y. Hwang, B. Batlogg, H. Takagi, H. L. Kao, R. J. Cava, J. J. Krajewski, and W. F. Peck, Jr., Phys. Rev. Lett. **72**, 2636 (1994).

[5] C. Allgeier and J. S. Schilling, Phys. Rev. B **48**, (1993); T. Kondo, Y. Kubo, Y. Shimakawa, and T. Manako, Phys. Rev. B **50**, 1244 (1994).

[6] Y. J. Uemura, G. M. Luke, B. J. Sternlieb, J. H. Brewer, J. F. Carolan, W. N. Hardy, R. Kadono, J. R. Kempton, R. F. Kiefl, S. R. Kreitzman, P. Mulhern, T. M. Riseman, D. Ll. Williams, B. X. Yang, S. Uchida, H. Takagi, J. Gopalakrishnan, W. A. Sleight, M. A. Subramanian, C. L. Chien, M. Z. Cieplak, Gang Xiao, V. Y. Lee, B. W. Statt, C. E. Stronach, W. J. Kossler, and X. H. Yu, Phys. Rev. Lett. **62**, 2317 (1989); Y. J. Uemura, L. P. Le, G. M. Luke, B. J. Sternlieb, W. D. Wu, J. H. Brewer, T. M. Riseman, C. L. Seaman, M. B. Maple, M. Ishikawa, D. G. Hinks, J. D. Jorgensen, G. Saito, and H. Yamochi, Phys. Rev. Lett. **66**, 2665 (1991).

[7] Ch. Niedermayer, C. Bernhard, U. Binninger, H. Glückler, J. L. Tallon, E. J. Ansaldo, and J. I. Budnick, Phys. Rev. Lett. **71**, 1764 (1993); *ibid.* **72**, 2502 (1994).

[8] J. L. Tallon and J. W. Loram, J. Supercond. **7**, 151 (1994).

[9] C. Bernhard, Ch. Niedermayer, U. Binninger, A. Hofer, J. L. Tallon, G. V. M. Williams, E. J. Ansaldo, and J. I. Budnick, Physica C **226**, 250 (1994).

[10] Y. J. Uemura, A. Keren, L. P. Le, G. M. Luke, W. D. Wu, Y. Kubo, T. Manako, Y. Shimakawa, M. Subramanian, J. L. Cobb, and J. T. Markert, Nature **364**, 605 (1993).

[11] B. Pümpin, H. Keller, W. Kündig, W. Odermatt, I. M. Savic, J. W. Schneider, E. Kaldis, S. Rusiecki, Y. Maeno, and C. Rossel, Phys. Rev. B **42**, 8019 (1990).

[12] D. H. Kim, K. E. Gray, R. T. Kampwirth, J. C. Smith, D. S. Richerson, T. J. Marks, J. H. Kang, J. Talvacchio, and M. Eddy, Physica C **177**, 431 (1991).

[13] J. L. Tallon, in *Proceedings of the 7th International Workshop on Critical Currents in Superconductors*, edited by H. W. Weber (World Scientific, Singapore, 1994), p. 52.

[14] T. Shibauchi, H. Kitano, K. Uchinokura, A. Maeda, T. Kimu-

ra, and K. Kishio, Phys. Rev. Lett. **72**, 2263 (1994).
[15]D. N. Basov, T. Timusk, B. Dabrowski, and J. D. Jorgensen, Phys. Rev. B **50**, 3511 (1994).
[16]J. L. Tallon, C. Bernhard, U. Binninger, A. Hofer, G. V. M. Williams, E. J. Ansaldo, J. I. Budnick, and Ch. Niedermayer, Phys. Rev. Lett. **74**, 1008 (1995).
[17]E. H. Brandt, Phys. Rev. Lett. **66**, 3213 (1991).
[18]D. R. Harshman and A. T. Fiory, Phys. Rev. Lett. **72**, 2501 (1994), and references therein.
[19]D. R. Harshman and A. P. Millis Jr., Phys. Rev. B **45**, 10 684 (1992).
[20]S. L. Lee, P. Zimmermann, H. Keller, M. Warden, I. M. Savic, R. Schauwecker, D. Zech, R. Cubitt, E. M. Forgan, P. H. Kes, T. W. Li, A. A. Menowsky, and Z. Tarnawski, Phys. Rev. Lett. **71**, 3862 (1993).
[21]E. H. Brandt, Phys. Rev. B **37**, 2349 (1988).
[22]D. Herlach, G. Majer, J. Major, J. Rosenkranz, M. Schmolz, W. Schwarz, A. Seeger, W. Templ, E. H. Brandt, U. Essmann, K. Fürderer, and M. Gladisch, Hyp. Int. **63**, 41 (1990).
[23]D. R. Harshman, L. F. Schneemayer, J. V. Waszczak, G. Aeppli, R. J. Cava, B. Batlogg, L. W. Rupp, E. J. Ansaldo, and D. Ll. Williams, Phys. Rev. B **39**, 851 (1989).
[24]T. M. Riseman, J. H. Brewer, K. H. Chow, W. N. Hardy, R. F. Kiefl, S. R. Kreitzman, R. Liang, A. MacFralane, P. Mendels, G. D. Morris, J. Rammer, and J. W. Schneider, Hyp. Int. **86**, 481 (1994); J. E. Sonier, R. F. Kiefl, J. H. Brewer, D. A. Bonn, J. F. Carolan, K. H. Chow, P. Dosanjh, W. N. Hardy, R. Liang, W. A. MacFarlane, P. Mendels, G. D. Morris, T. M. Riseman, and J. W. Schneider, Phys. Rev. Lett. **72**, 744 (1994).
[25]W. Bardford and J. M. F. Gunn, Physica C **156**, 515 (1988).
[26]A. J. Greer, W. J. Kossler, and K. G. Petzinger, Hyp. Int. **86**, 531 (1994).
[27]J. L. Tallon and G. V. M. Williams, Phys. Rev. B (to be published).
[28]J. L. Tallon (private communication).
[29]J. L. Tallon, C. Bernhard, H. Shaked, R. L. Hitterman, and J. D. Jorgensen, Phys. Rev. B **51**, 12 911 (1995).
[30]T. Wada, Y. Yaegashi, A. Icinose, H. Yamauchi, and S. Tanaka, Phys. Rev. B **44**, 2341 (1991).
[31]P. P. Hyguen, Z. H. Wang, A. M. Rao, M. S. Dresselhaus, J. S. Moodera, G. Dresselhaus, H. B. Radousky, R. S. Glass, and J. Z. Liu, Phys. Rev. B **48**, 1148 (1993).
[32]T. G. N. Babu and C. Greaves, Physica C **207**, 44 (1993).
[33]H. Lütgemeier, I. Heinmaa, D. Wagener, and S. M. Hosseini, in *Proceedings of the Workshop Phase Separation in Cuprate Superconductors,* Cottbus 1993, edited by E. Sigmund and K. A. Müller (Springer-Verlag, Berlin, 1993).
[34]E. J. Ansaldo, Ch. Niedermayer, J. L. Tallon, D. M. Pooke, J. H. Brewer, G. D. Morris, and S. R. Kreitzman, Physica C **185-189**, 1763 (1991).
[35]E. J. Ansaldo, J. J. Boyle, Ch. Niedermayer, H. Glückler, J. L. Tallon, A. Mawdsley, D. Pooke, C. E. Stronach, D. R. Noakes, R. S. Carry, M. R. Davis, and G. D. Morris, Hyp. Int. **86**, 505 (1994).
[36]R. Cubitt, E. M. Forgan, M. Warden, S. L. Lee, P. Zimmermann, H. Keller, I. M. Savic, P. Wenk, D. Zech, P. H. Kes, T. W. Li, A. A. Menowsky, and Z. Tarnawski, Physica C **213**, 126 (1993).
[37]K. Kishio, J. Shimoyama, Y. Kotaka, and K. Yamafuji, in *Proceedings of the 7th International Workshop on Critical* Currents in Superconductors, edited by H. W. Weber (World Scientific, Singapore, 1994), p. 339.
[38]C. Bernhard, C. Wenger, Ch. Niedermayer, D. M. Pooke, J. L. Tallon, Y. Kotaka, J. Shimoyama, K. Kishio, D. R. Noakes, C. E. Stronach, T. Sembiring, and E. J. Ansaldo, Phys. Rev. B **52**, 7050 (1995).
[39]V. Hardy, A. Wahl, A. Ruyter, A. Maigan, C. Martin, L. Coudrier, J. Provost, and Ch. Simon, Physica C **232**, 347 (1994).
[40]W. J. Kossler, X. H. Yu, A. Greer, H. E. Schone, C. E. Stronach, M. Davis, R. S. Carry, W. F. Lankford, and J. Oostens, Hyp. Int. **63**, 81 (1990); C. Bucci, P. Carretta, R. De Renzi, G. Guidi, F. Licci, L. G. Raffo, H. Keller, S. Lee, and I. M. Savic, Physica C **235-240**, 1849 (1994).
[41]Y. Kubo, Phys. Rev. B **50**, 3181 (1994).
[42]T. Schneider and M. H. Pedersen, J. Supercond. **7**, 593 (1994).
[43]B. Pümpin, H. Keller, W. Kündig, I. M. Savic, J. W. Schneider, H. Simmler, and P. Zimmermann, Hyp. Int. **63**, 26 (1990).
[44]A. J. Vega, W. E. Farneth, E. M. McCarron, and R. K. Bordia, Phys. Rev. B **39**, 2322 (1989).
[45]J. Buan, B. Zhou, C. C. Huang, J. Z. Liu, and R. N. Shelton, Phys. Rev. B **49**, 12 220 (1994).
[46]Z. Schlesinger, R. T. Collins, F. Holtzberg, C. Field, S. H. Blanton, U. Welp, G. W. Grabtree, Y. Fang, and J. Z. Liu, Phys. Rev. Lett. **65**, 801 (1990).
[47]A. Zibolt, L. Widder, H. P. Geserich, G. Bräuchle, H. Claus, H. v. Löhneysen, N. Nücker, A. Erb, and G. Müller-Voigt, Physica C **212**, 365 (1993).
[48]M. Knupfer, G. Roth, J. Fink, J. Karpinski, and E. Kaldis, Physica C **230**, 121 (1994), and references therein.
[49]J. L. Cohn, E. F. Skelton, S. A. Wolf, and J. Z. Liu, Phys. Rev. B **45**, 13 140 (1992).
[50]T. A. Friedmann, M. W. Rabin, J. Giapintzakis, J. P. Rice, and D. M. Ginsberg, Phys. Rev. B **42**, 6217 (1990); B. Bucher, P. Steiner, J. Karpinski, E. Kaldis, and P. Wachter, Phys. Rev. Lett. **70**, 2012 (1993); R. Gagnon, C. Lupien, and L. Taillefer, Physica C **235-240**, 1409 (1994).
[51]P. B. Allen, W. E. Pickett, and H. Krakauer, Phys. Rev. B **37**, 7482 (1988); S. Massida, J. Yu, K. T. Park, and A. J. Freeman, Physica C **176**, 159 (1991); J. Yu, S. Massida, A. J. Freeman and R. Podloucky, Physica C **214**, 335 (1993); J. Kircher, M. Cardona, A. Zibold, H. P. Geserich, E. Kaldis, J. Karpinski, and S. Rusiecki, Phys. Rev. B **48**, 3993 (1993).
[52]V. Z. Kresin and S. A. Wolf, Phys. Rev. B **46**, 6458 (1992); V. Z. Kresin and S. A. Wolf, J. Supercond. **7**, 531 (1994).
[53]K. Zhang, D. A. Bonn, S. Kamal, R. Liang, D. J. Baar, W. N. Hardy, D. N. Basov, and T. Timusk, Phys. Rev. Lett. **73**, 2484 (1994); D. N. Basov, R. Liang, D. A. Bonn, W. N. Hardy, B. Dabrowski, M. Quijada, D. B. Tanner, J. P. Rice, D. M. Ginsberg, and T. Timusk, Phys. Rev. Lett. **74**, 598 (1995).
[54]V. Breit, P. Schweiss, R. Hauff, H. Wühl, H. Claus, H. Rietschel, A. Erb, and G. Müller-Voigt (unpublished).
[55]K. Conder, S. Rusiecki, and E. Kaldis, Mater. Res. Bull. **24**, 581 (1989).
[56]J. L. Tallon, Physica C **168**, 85 (1990).